Journal of Catalysis 281 (2011) 309–317

Contents lists available at ScienceDirect

Journal of Catalysis

journal homepage: www.elsevier.com/locate/jcat

Photocatalytic decomposition of ethanol on TiO_2 modified by N and promoted by metals

Gyula Halasi, Imre Ugrai, Frigyes Solymosi *

Reaction Kinetics Research Group, Chemical Research Center of the Hungarian Academy of Sciences, Department of Physical Chemistry and Materials Science, University of Szeged, P.O. Box 168, H-6701 Szeged, Hungary

ARTICLE INFO

Article history:
Received 8 April 2011
Revised 12 May 2011
Accepted 12 May 2011
Available online 15 June 2011

Keywords:
Photodecomposition of ethanol
TiO_2 photocatalyst
N-doped TiO_2
Rh and Ag promoted TiO_2

ABSTRACT

The photo-induced vapor-phase decomposition of ethanol was investigated on pure, N-doped, and metal-promoted TiO_2. The catalysts were characterized by bandgap determination and by FTIR and XPS spectroscopy. In harmony with previous findings, the bandgap of N-doped TiO_2 continuously decreased from 3.15 to 2.17 eV with elevation of the temperature of its modification. IR studies revealed that illumination of the C_2H_5OH–TiO_2 system initiated the decomposition of adsorbed ethoxy species to yield acetaldehyde. The photodecomposition of ethanol on pure TiO_2 occurs to only a very limited extent; N-doped TiO_2 displays much higher activity and gives acetaldehyde and hydrogen as the primary products. The acetaldehyde formed is photolyzed to afford methane and CO. The efficiency of the N-doped TiO_2 increased with the narrowing of the bandgap, a feature attributed to the prevention of electron–hole recombination. The deposition of Rh on pure and doped TiO_2 dramatically enhanced the extent of photodecomposition of ethanol, even in visible light.

1. Introduction

Great efforts are currently being made to produce hydrogen for fuel and for various other applications. Oxygenated hydrocarbons (methanol, ethanol, and dimethyl ether) are the most generally and conveniently used sources of hydrogen production [1–3]. A number of effective materials have been developed for the catalysis of their decomposition and reforming. Unfortunately, even on the most effective and expensive Pt metals [4–17] and on the much less expensive Mo_2C [18,19], the reactions of these oxygenated hydrocarbons occur at relatively high temperatures. Their photocatalytic decomposition may provide a solution, as in this way hydrogen might be generated even at ambient temperature. Of the semiconductors, TiO_2 is applied frequently as a photocatalyst. However, its wide bandgap (3.0–3.2 eV) requires the use of UV light during the reactions, as only 4–5% of solar energy can be utilized for photoreactions. In contrast with heterogeneous catalysis, where the catalytic efficiency of TiO_2 can be varied appreciably by altervalent cations [20,21], in photocatalysis, anionic dopants have been found to be effective due to the narrowing of the bandgap of TiO_2, leading to visible light photocatalysis [22–29]. Over the past 20 years, a tremendous amount of work has been devoted to photocatalysis, including the photolysis of ethanol (for reviews, see [30–32]). Most of the published studies have dealt with the oxidation of ethanol generated as a pollutant by industry, or automobiles fueled by ethanol, and much less with the aim of producing hydrogen [33–44]. The present paper reports on the photodecomposition of ethanol on TiO_2 modified with N and on the effects of Rh, one of the most active metals for the decomposition of ethanol [4–6,9,12–17]. Measurements were also carried out with Ag/TiO_2, which exhibited high activity in the reduction of NO with ethanol in heavily oxidizing exhaust gas [45–47]. Its catalytic efficiency was earlier found to be greatly increased by illumination with a 15 W germicide lamp [48].

2. Experimental

2.1. Materials

Two types of TiO_2 were used: Degussa, P 25 (50 m^2/g) and Hombikat, UV 100 (300 m^2/g). For the preparation of N-doped TiO_2, we applied several methods. Following the description of Beranek and Kisch [28], titania powder was placed into 230-ml Schlenk tube connected via an adapter with 100-ml round-bottom flask containing 1 g of urea and heated in a muffle furnace for 30 min at different temperatures [28]. Samples prepared by this general method are denoted with "SK". In other cases, TiO_2 was treated with NH_3. Following the method of Yates et al. [27], Hombikat TiO_2 powder was heated in a flow reactor system in an argon gas atmosphere up to 870 K. The heating rates were 7 K/min. For doping, the argon flow was replaced by NH_3 for 30 min, after the target temperature had been reached. Subsequently, the

* Corresponding author. Fax: +36 62 544 106.
E-mail address: fsolym@chem.u-szeged.hu (F. Solymosi).

0021-9517/$ - see front matter © 2011 Elsevier Inc. All rights reserved.
doi:10.1016/j.jcat.2011.05.016

powder was kept in flowing argon for 1 h at 870 K and then cooled in flowing argon over a time period of 2–3 h to room temperature. This sample was marked "SY". N-modified TiO_2 sample (named "SX") was also produced following the description of Xu et al. [25]. Titanium tetrachloride was used as a precursor. After several steps, the NH_3-treated TiO_2 slurry was vacuum dried at 353 K for 12 h, followed by calcination at 773 K in flowing air for 3 h. Ag/TiO_2 and Rh/TiO_2 samples were prepared by impregnation of pure and various N-doped titania in the solution of $AgNO_3$ or $RhCl_3$. The suspension was dried at 373 K and annealed at 573 K for 1 h. For IR studies, the dried samples were pressed in self-supporting wafers (30×10 mm $\sim$10 mg/cm^2). For photocatalytic measurements, the sample (70–80 mg) was sprayed onto the outer side of the inner quartz tube of the catalytic reactor from aqueous suspension. The surface of the catalyst film was 168 cm^2. The catalysts were oxidized at 573 K and reduced at 573 K in the IR cell or in the catalytic reactor in O_2 or H_2 stream for 1 h. The dispersion of Rh was determined by H_2 adsorption at 300 K. We obtained a value of 26.6%. Ethanol with purity of 99.7% was supplied by Sharlau.

2.2. Methods

Diffuse reflectance spectra of TiO_2 samples were obtained relative to the reflectance of a standard ($BaSO_4$) using an UV/Vis spectrophotometer (OCEAN OPTICS, Typ.USB 2000) equipped with a diffuse reflectance accessory. The samples were pressed pellets of a mixture of 2 g of $BaSO_4$ with 50 mg of the powder. X-ray photoelectron spectroscopy (XPS) measurements were performed with a Kratos XSAM 800 instrument, using non-monochromatic Al Kα radiation ($h\nu$ = 1486.6 eV) and a 180° hemispherical analyzer at a base pressure of 1×10^{-9} mbar. Binding energies were referenced to the C1s binding energy (BE) (285.1 eV). The surface area of the catalysts was determined by application of the BET method with N_2 adsorption at $\sim$100 K. Data are listed in Table 1. For FTIR studies, a mobile IR cell housed in a metal chamber was used. The sample can be heated and cooled to 150–200 K in situ. The IR cell can be evacuated to 10^{-5} Torr using a turbo molecular pumping system. The samples were illuminated by the full arc of a Hg lamp (LPS-220, PTI) outside the IR sample compartment. The IR range of the light was filtered by a quartz tube (10 cm length) filled with triply distilled water applied at the exit of the lamp. The filtered light passed through a high-purity CaF_2 window into the cell. The light of the lamp was focused onto the sample. The output produced by this setting was 300 mW cm^{-2} at a focus of 35 cm. The maximum photon energy at the sample is ca. 5.4 eV (the onset of UV intensity from the lamp). After illumination, the IR cell was moved to its regular position in the IR beam. Infrared spectra were recorded with a Biorad (Digilab. Div. FTS 155) instrument with a wavenumber accuracy of ±4 cm^{-1}. All the spectra presented in this study are difference spectra.

Photocatalytic reaction was followed in a thermostatically controllable photoreactor equipped with a 15 W germicide lamp (type GCL 307T5L/CELL, Lighttech Ltd., Hungary) as light source. This lamp emits predominantly in the wavelength range of 250–440 nm. Its maximum intensity is at 234 nm. For the visible photocatalytic experiments, another type of lamp was used (Lighttech GCL 307T5L/GOLD) with 400–640 nm wavelength range and two maximum intensities at 453 and 545 nm. We note that this lamp also emits below 400 nm. The approximate light intensity at the catalyst films is 3.9 mW/cm^2 for the germicide lamp and 2.1 mW/cm^2 for the other lamp. The reactor (volume: 970 ml) consists of two concentric Pyrex glass tubes fitted one into the other and a centrally positioned lamp. It is connected to a gas-mixing unit serving for the adjustment of the composition of the gas or vapor mixtures to be photolyzed in situ. The length of the concentric tubes was 250 mm. The diameter of outer tube was 70 mm and that of the inside tube 28 mm. The width of annulus between them was 42 mm, and that of the photocatalyst film was 89 mm. Ethanol ($\sim$1.3%) was introduced in the reactor through an externally heated tube avoiding condensation. The carrier gas was Ar, which was bubbled through ethanol at room temperature. The gas-mixture was circulated by a pump. The reaction products were analyzed with a HP 5890 gas chromatograph equipped with PORAPAK Q and PORAPAK S packed columns. The sampling loop of the GC was 500 μl.

Table 1
Some characteristic data for pure and N-modified TiO_2.

Sample	Pretreatment temperature (K)	Surface area (m^2/g)	Bandgap (eV)	Notation
TiO_2	As received	200	3.17	Hombikat
TiO_2	723	135		
TiO_2 + N	573	115	3.15	Prepared by Kisch et al. (SK) [28]
TiO_2 + N	673	96	2.35	
TiO_2 + N	723	90	2.15	
TiO_2 + N	773	81	2.17	
TiO_2	870	54.5		Hombikat
TiO_2 + N	870	53	3.12	Prepared by Yates et al. (SY) [27]
TiO_2	723	265	3.00	Prepared by Xu et al. (SX) [25]
TiO_2 + N	723	79	1.96	

3. Results and discussion

3.1. Characterization of the catalysts

Fig. 1 presents plots of the Kubelka–Munk function $F(R_\infty)$ *vs.* wavelength, obtained from diffuse reflectance data. Similarly, as observed by Beranek and Kisch [28], the color changed from yellowish to intense yellow and orange on increase of the pretreatment temperature. Correspondingly, the absorption edge shifted significantly to the visible range. In the determination of bandgap energies, E_g, we followed the calculation procedure of Beranek and Kisch [28], who used the equation $\alpha = A(h\nu - E_g)^n/h\nu$, where α is the absorption coefficient, A is a constant, $h\nu$ is the energy of light, and n is a constant depending on the nature of the electron transition [49]. Assuming an indirect bandgap (n = 2) for TiO_2 [50], with α proportional to $F(R_\infty)$, the bandgap energy can be obtained from the plots of $[F(R_\infty)h\nu]^{1/2}$ *vs.* $h\nu$, as the intercept at $[F(R_\infty)h\nu]^{1/2} = 0$ of the extrapolated linear part of the plot (Fig. 1). The bandgap for pure TiO_2 was 3.17 eV, while that for N-doped TiO_2 sintered at 573 K was slightly less and continuously decreased to 2.17 ± 0.03 eV with increase in the temperature of its modification. We did not perform elemental analysis, but the results of Beranek and Kisch [28] revealed that beside N, its maximum amount was 11.8% in the sample modified 773 K, carbon has been also incorporated in the surface layer of TiO_2. Accordingly, this C also contributes to the lowering of the bandgap of TiO_2. We found smaller red shifts for N-doped TiO_2 prepared by the reaction of TiO_2 with NH_3 (Table 1).

N-doped TiO_2 (sample SK) was also examined by FTIR measurements. The spectrum revealed that several adsorbed species remained on the solid surface after preparation, yielding intense absorption bands in the ranges 1900–2300 and 1300–1700 cm^{-1} (Fig. 2A). The positions of the bands and their intensities were very sensitive to the preparation of the samples. As shown in Fig. 2B, they could not be eliminated by treating the sample with oxygen at different temperatures; moreover, the band at 2186–2199 cm^{-1} intensified somewhat on treatment up to 573 K and decayed considerably only at 673 K. At the same time, the color of the sample

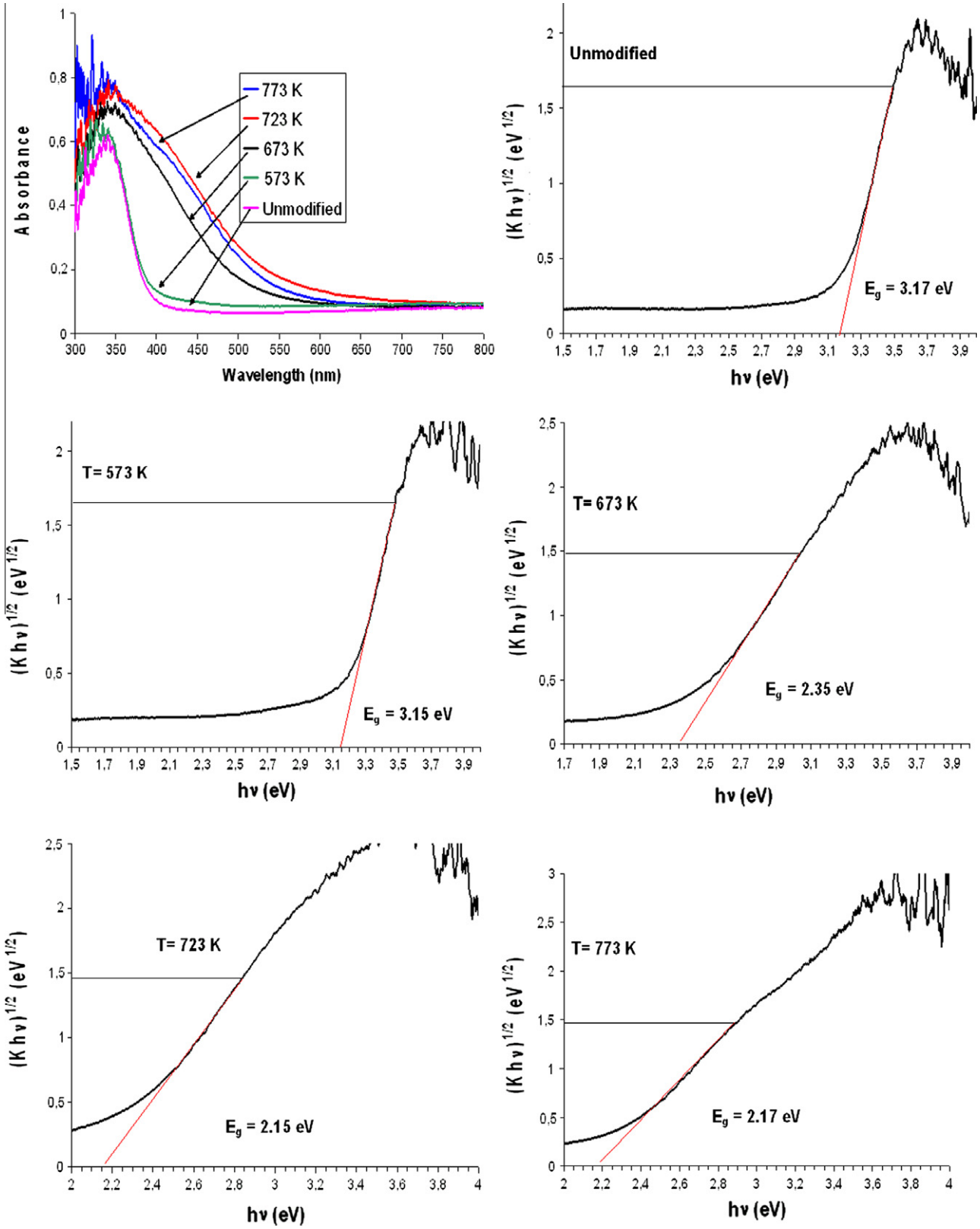

Fig. 1. Plots of Kubelka–Munk function *vs.* wavelength of powders modified at different temperatures (A) and bandgap determination using $[F(R_\infty)h\nu]^{1/2}$vs. $h\nu$ plots (assuming indirect optical transition) for unmodified TiO_2 and TiO_2–N modified at different temperatures.

progressively changed from yellow to orange and brown. The intense absorption bands are very probably due to isocyanate, cyanide, and other products of the pyrolysis of urea. Their formation and presence were also considered in the original paper describing the preparation [28]. The characteristic absorption band of NCO bound to TiO_2 is situated at 2205–2210 cm^{-1}, and that of CN is at

2090–2150 cm^{-1} [51]. Both surface species, and particularly the CN group, are very stable on TiO_2. The absorption feature at ~1618 cm^{-1} is very likely due to δ_{as} vibration of NH groups.

Since the first preparation of N-doped TiO_2, it has been subjected to extensive XPD and XPS studies [22–29]. The nature of the incorporated N and its place in the TiO_2 lattice are still debated. It is not a purpose of the present paper to contribute to this debate. Nevertheless, for the characterization of our samples, we also performed informative XPS measurements. We found only slight shifts in the binding energies (BE) of Ti2p and N1s on the XPS spectra of N-doped TiO_2 (sample SK) prepared at different temperatures. These results are in good agreement with those obtained previously [28]. Treatment of the N-doped TiO_2 in vacuum at various temperatures resulted in very minor changes in the XPS spectrum. As the IR studies revealed a considerable amount of carbon-containing compounds on the surface, we also examined the influence of oxygen treatment on the XPS spectrum of TiO_2 + N (SK, 673 K). Spectra obtained after oxidation at different temperatures are displayed in Fig. 3. The binding energy (BE) for $Ti2p_{2/3}$ at 459.0 eV shifted slightly to lower energy with elevation of the temperature (Fig. 3A). The BE for N1s also moved lower with the temperature (Fig. 3B). In the C1s region, a very intense peak was observed at 285.1 eV and a shoulder at 288.0 eV, supporting the presence of carbon in the surface layer (Fig. 3C). A considerable decay in the BE of C1s 288.0 eV occurred only at 673 K.

3.2. FTIR study of photolysis of ethanol

The interaction of ethanol with TiO_2 has been extensively studied by IR spectroscopy, and the effect of illumination of the system of $C_2H_5OH + O_2$ over TiO_2 has likewise been thoroughly examined [39]. The adsorption of ethanol on pure TiO_2 produced intense absorption bands in the IR spectrum (Fig. 4A), which can be attributed to the vibrations of adsorbed ethoxy species (Table 2). As a result of irradiation, a broad weak band developed between 1500 and 1600 cm^{-1}, which can be separated into two peaks at 1549 and 1579 cm^{-1}. The first is ascribed to ν_{as}(COO) vibration of adsorbed acetate and the second one to ν_{as} of formate (Table 2). Note that there was no peak at 1718–1723 cm^{-1} due to acetaldehyde. Similar measurements were carried out with N-doped TiO_2 (sample SK, 673 K). The positions of the bands in the C—H stretching vibration region remained the same. In the interval 1500–1600 cm^{-1} vibration bands appeared at 1551 and 1584 cm^{-1} (Fig. 4B).

More dramatic spectral changes occurred when Rh was deposited on TiO_2. In order to avoid the disturbance caused by the absorption bands in the region 2000–2300 cm^{-1} for the N-doped TiO_2 prepared by the decomposition of urea, experiments were performed with the sample SY. Spectra are presented in Fig. 4C. In the high-frequency region, almost the same absorption bands were observed as for pure TiO_2. Additionally, however, relatively strong CO bands due to linearly bonded CO (Rh_x–CO) and bridging CO (Rh_2–CO) appeared at 2008 and 1837 cm^{-1} even without illumination; their intensities increased appreciably as a consequence of irradiation. There was no sign of the absorption bands at 2030 and 2100 cm^{-1}, indicative of the formation of $Rh^+(CO)_2$ as a result of the oxidative disruption of Rh nanoparticles [52]. A possible reason is that the H_2 formed prevented this process [52]. Similar spectral features were experienced for Rh deposited on sample SY (Fig. 4D). In the low-frequency range, the picture was the same as for TiO_2. In order to eliminate the thermal effect, measurements were repeated at ~200 K. Without irradiation, no absorption features were registered between 1800 and 2150 cm^{-1}. Even at the beginning of the photolysis, however, a well-detectable peak due to adsorbed CO appeared at 2045 cm^{-1}. Its absorbance slightly increased with elevation of the duration of irradiation.

3.3. Photocatalytic decomposition on pure and N-doped TiO_2

The results obtained following the photolysis of ethanol on pure TiO_2 are displayed in Fig. 5A. Even at room temperature, illumination initiated the decomposition of ethanol, to give acetaldehyde, hydrogen, methane, and CO as the major products. The predominant reaction pathway was clearly dehydrogenation. The conversion of ethanol was very low: ~4% in 240 min. The results were well reproducible in the repeated measurements. Previous [39] and the present IR studies have clearly revealed that ethanol readily dissociates on TiO_2 to give adsorbed ethoxy species even at room temperature:

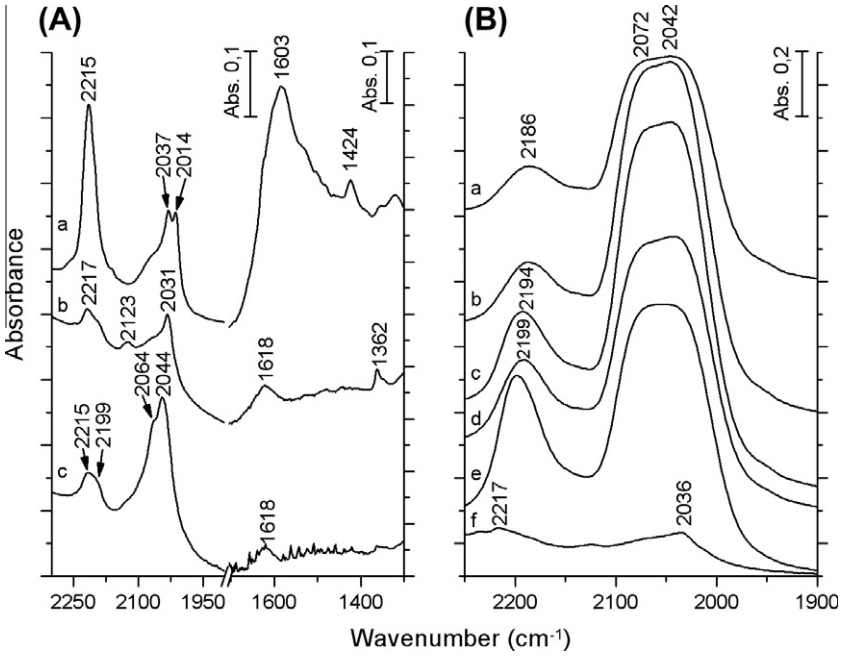

Fig. 2. (A) FTIR spectra of TiO_2 + N (SK) modified at 573 K (a), 673 K (b), and 773 K (c). (B) Effects of oxidation of TiO_2 + N modified at 673 K. Unoxidized (a); 300 K (b); 373 K (c); 473 K (d); 573 K (e); 673 K (f).

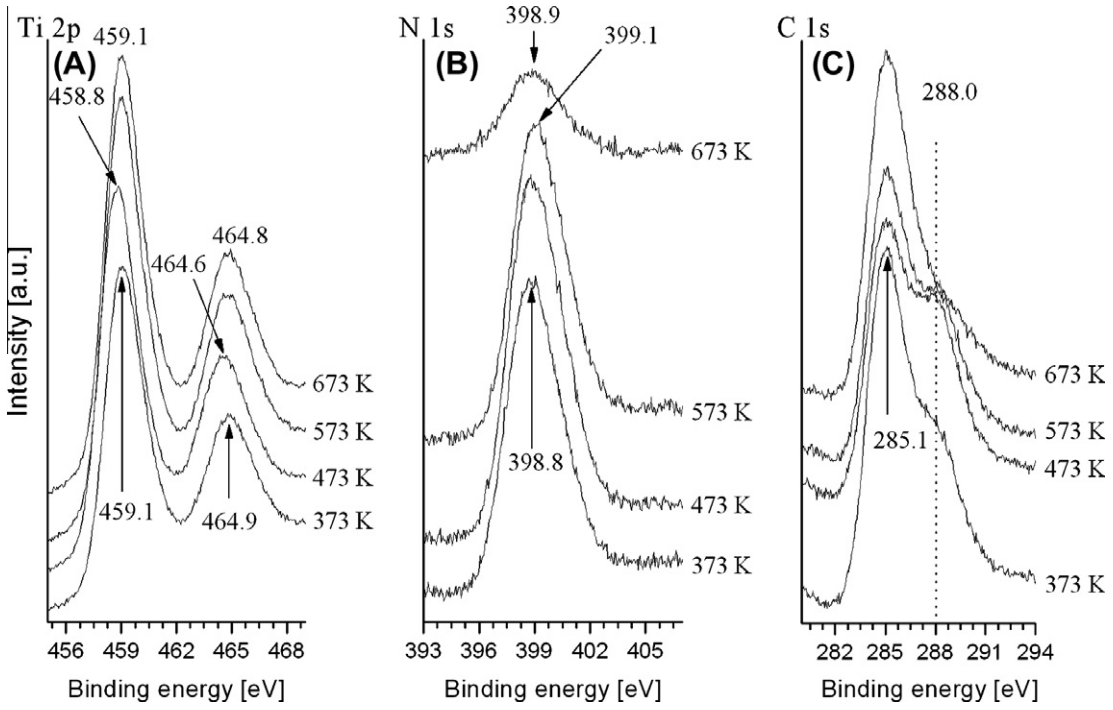

Fig. 3. Effects of O_2 treatment on the XPS spectra of N-doped TiO_2 (SK) modified at 673 K. The sample was kept in O_2 stream (flow rate 40 ml/min) in the preparation chamber at different temperatures for 60 min. Afterward, it was transferred into the analyzing chamber.

$$C_2H_5OH_{(g)} = C_2H_5OH_{(a)} \quad (1)$$

$$C_2H_5OH_{(a)} = C_2H_5O_{(a)} + H_{(a)} \quad (2)$$

This process does not need illumination. As only traces of acetaldehyde were detected on pure TiO_2 without irradiation, it may be assumed that the slow step in the dehydrogenation of ethanol to acetaldehyde and hydrogen is the decomposition of ethoxy species or more precisely the cleavage of one of the C—H bonds. Photolysis of the C_2H_5OH–TiO_2 system, however, initiated the decomposition of ethoxy on TiO_2, very probably involving the donation of a photoelectron formed in the photo-excitation process:

$$TiO_2 + h\nu = h^+ + e^- \quad (3)$$

to the ethoxy species:

$$C_2H_5O_{(a)} + e^- = C_2H_5O^{\delta-}_{(a)} \quad (4)$$

This step is followed by the photo-induced decomposition of ethoxy to acetaldehyde and hydrogen:

$$C_2H_5O^{\delta-}_{(a)} = CH_3CHO^{\delta-}_{(a)} + H_{(a)} \quad (5)$$

The adsorbed hydrogen may reduce the TiO_2 surface or react with surface oxygen to yield OH. In the case of TiO_2 samples, it was a general observation that the amount of H_2 was much less than that of acetaldehyde. We assume that beside the reduction process, a fraction of H_2 reacts with the surface species produced by the preparation of TiO_2 + N samples. The formation of CH_4 and CO suggests the further decomposition of acetaldehyde:

$$CH_3CHO^{\delta-}_{(a)} = CH_4 + CO^{\delta-}_{(a)} \quad (6)$$

$$CO^{\delta-}_{(a)} + h^+ = CO_{(g)} \quad (7)$$

This is a photo-catalyzed process as acetaldehyde does not decompose on TiO_2 at this temperature. The tiny amounts of ethylene and ethane in the products suggest that the dehydration of ethanol

$$C_2H_5OH = C_2H_4 + H_2O \quad (8)$$

and the resulting hydrogenation of ethylene to ethane

$$C_2H_4 + H_2 = C_2H_6 \quad (9)$$

occur to only negligible extents. The level of photolysis on pure TiO_2 is very low, most likely because of the ready recombination between electrons and holes generated by light.

The incorporation of N into TiO_2 (sample SK), however, appreciably increased the extent of photodecomposition, as indicated by the higher conversion and rates of product formation (Fig. 5B,C). With the consumption of ethanol, formation of acetaldehyde apparently slowed down or even ceased. At the same time, more CH_4 and CO were produced on longer illumination, indicating the occurrence of the photodecomposition of acetaldehyde (Eq. (5)). The effect of doping TiO_2 with N depended on the pretreatment. Both the conversion and the product distribution increased with increase in the temperature of modification of N-doped TiO_2. The highest photocatalytic activity was exhibited by the sample annealed at 773 K. When the surface area of the sample was taken into account, this effect was more pronounced (Fig. 5D). In view of the change in the bandgap of N-doped TiO_2 with the modification temperature (Fig. 1), it may be concluded that the extent of photolysis of ethanol on TiO_2 is markedly enhanced by the narrowing of the bandgap of TiO_2. This can be explained by the prevention of electron–hole recombination.

As the narrowed bandgap allows TiO_2 to absorb light at lower wavelengths, measurements were performed with the use of a lamp emitting in the visible range. These experiments were carried out with TiO_2 (SX), which possesses better performance. The results presented in Fig. 6A and B show that, whereas pure TiO_2 exhibits moderate activity in the visible light, the photoactivity of N-doped sample (SX) is significantly higher.

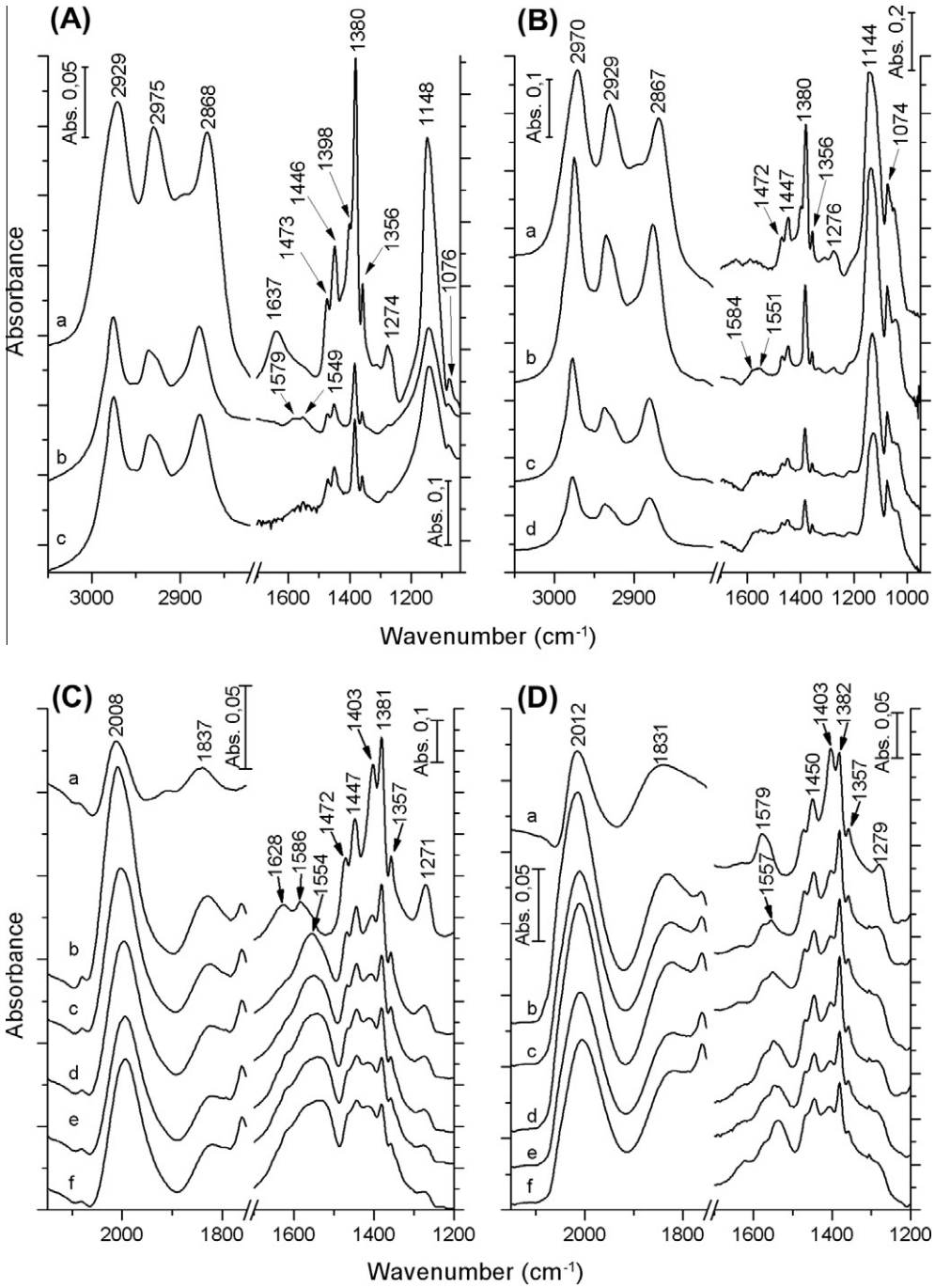

Fig. 4. Effects of illumination time on the FTIR spectra of adsorbed ethanol on pure TiO_2 (A), N-doped TiO_2 (SK, 773 K) (B), Rh/TiO_2 (C), and Rh/TiO_2 + N (SY, 773 K) (D) at 300 K. Illumination was performed in ethanol vapor. From time to time, the irradiation was interrupted and spectral changes were registered at 300 K. All the spectra are difference spectra.

3.4. Effects of Rh and Ag

In further experiments, we examined the effects of the deposition of Rh on TiO_2 on the photodecomposition of ethanol. Results are shown in Fig. 7. Whereas the conversion of ethanol in 200 min on pure TiO_2 was less than 4.0%, in the presence of 2% Rh, it attained 90%. The dehydrogenation of ethanol remained the main reaction pathway. In this case, the amount of hydrogen greatly exceeded that of acetaldehyde, which reached a constant level at around ~140 min, when its photodegradation to methane and CO became more pronounced. The amounts of these two compounds increased as the duration of illumination was lengthened. Very small amounts of ethane and CO_2 were also detected. The deposition of Ag on TiO_2 similarly significantly promoted the photoreaction, but its effect was less than that of Rh.

As concerns the explanation of the effect of Rh, it should be borne in mind that Rh is a very active catalyst for the thermal decomposition of ethanol at higher temperature [4–6,9,12–17]. This is attributed to promotion of the rupture of a C—H bond in the ethoxy species adsorbed on Rh. Although the catalyst sample was cooled during the photolysis, the possibility cannot be excluded that the illumination caused a temperature rise of the catalyst. In order to check this possibility, a thin thermocouple was attached to the catalyst layer. The temperature rose by only a

Table 2
IR vibrational frequencies and their assignments for ethoxy, acetate, and formate species produced following the illumination of ethanol on TiO_2 catalysts at 300 K.

Vibrational mode	TiO_2 [39]	TiO_2 (SK) [present work]	TiO_2 + N (SK, 773 K) [present work]
Ethoxy			
$\nu_{as}(CH_3)$	2971	2975	2970
$\nu_{as}(CH_2)$	2931	2929	2929
$\nu_s(CH_3)$	2782, 2689	2868	2807
$\delta_{as}(CH_2)$	1450	1446	1447
$\delta_s(CH_2)$	1380	1380	1380
$\omega(CH_2)$	1356	1356	1356
ν(OC) mono-dentate	1147, 1113	1148	1144
ν(OC)/ν(CC)	1052	1076	1074
ν(OC) bi-dentate			
Acetate			
CH_3COO^- ν_{as}(COO)	1542	1549	1551
	1537		
$\delta_{as}(CH_3)$	1469		
ν_s	1446	1473	
	1443	1446	
	1438		
	1421		
$\delta_s(CH_3)$	1340		1356
Formate			
$HCOO^-$ ν_{as}(COO)	1581	1579	1584
δ(CH)	1416		
ν_s(COO)	1350	1380	

few degrees during illumination. We also examined the thermal reaction on the Rh-promoted TiO_2 layer used for photolysis without illumination and detected merely very slight decomposition (~1–2%) at 300 K. A measurable decomposition of ethanol (~3% in 60 min) was observed only at 423 K. The results of these control experiments lead us to exclude the contribution of thermal effects to the decomposition of ethanol induced by photolysis.

The dramatic influence of Rh was also investigated on N-doped TiO_2 in visible light. It was accepted that the incorporation of N into TiO_2 enhances its absorbance from solar light, and measurements were performed with a lamp emitting at 400–640 nm. Fig. 6C and D depict the photocatalytic effects of Rh deposited on pure TiO_2 and on N-doped TiO_2 (sample SY). A comparison immediately reveals that the photoactivity of the N-doped sample is clearly higher than that of Rh/TiO_2 free of nitrogen. This is reflected in the conversion of ethanol, in the amounts of the products of dehydrogenation, and in the photo-induced decomposition of acetaldehyde into CH_4 and CO.

The promoting effect of metal deposition on TiO_2 has been observed in a number of photoreactions, including the photo-oxidation of ethanol [53–55]. This effect was explained by a better separation of charge carriers induced by illumination and by improved electronic communication between metal particles and TiO_2 [53–55]. We believe that the electronic interaction between the metal and n-type TiO_2 plays an important role in the enhanced photoactivity of Rh/TiO_2, as demonstrated in the hydrogenation of CO and CO_2 [56] and in the photocatalytic reaction between H_2O and CO_2 [57]. As the work function of TiO_2 (~4.6 eV) is less than that of Rh (4.98 eV), electron transfer occurs from TiO_2 to Rh, which increases the activation of CO_2 in the form of CO_2^-. The role of such electronic interaction in the activity of a supported metal catalyst was first established in the case of the decomposition of formic

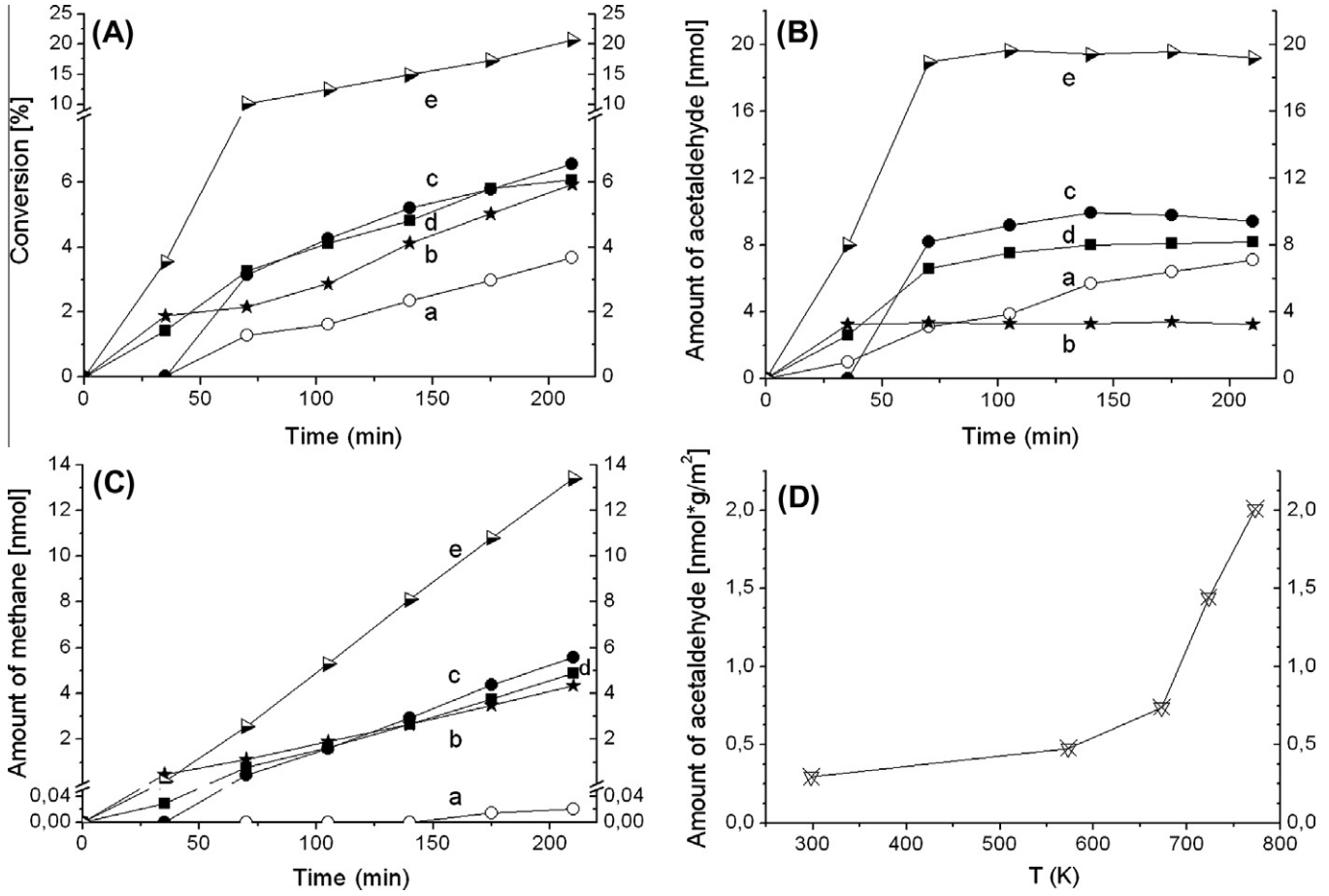

Fig. 5. Effects of pretreatment temperature of N-doped TiO_2 (SK) on the conversion of ethanol (A) and on the formation of acetaldehyde (B) and CH_4 (C). Rate of formation of acetaldehyde related to the surface area of the samples (D). Undoped TiO_2 (a); N-modified TiO_2 at 573 K (b); 673 K (c); 723 K (d); 773 K (e).

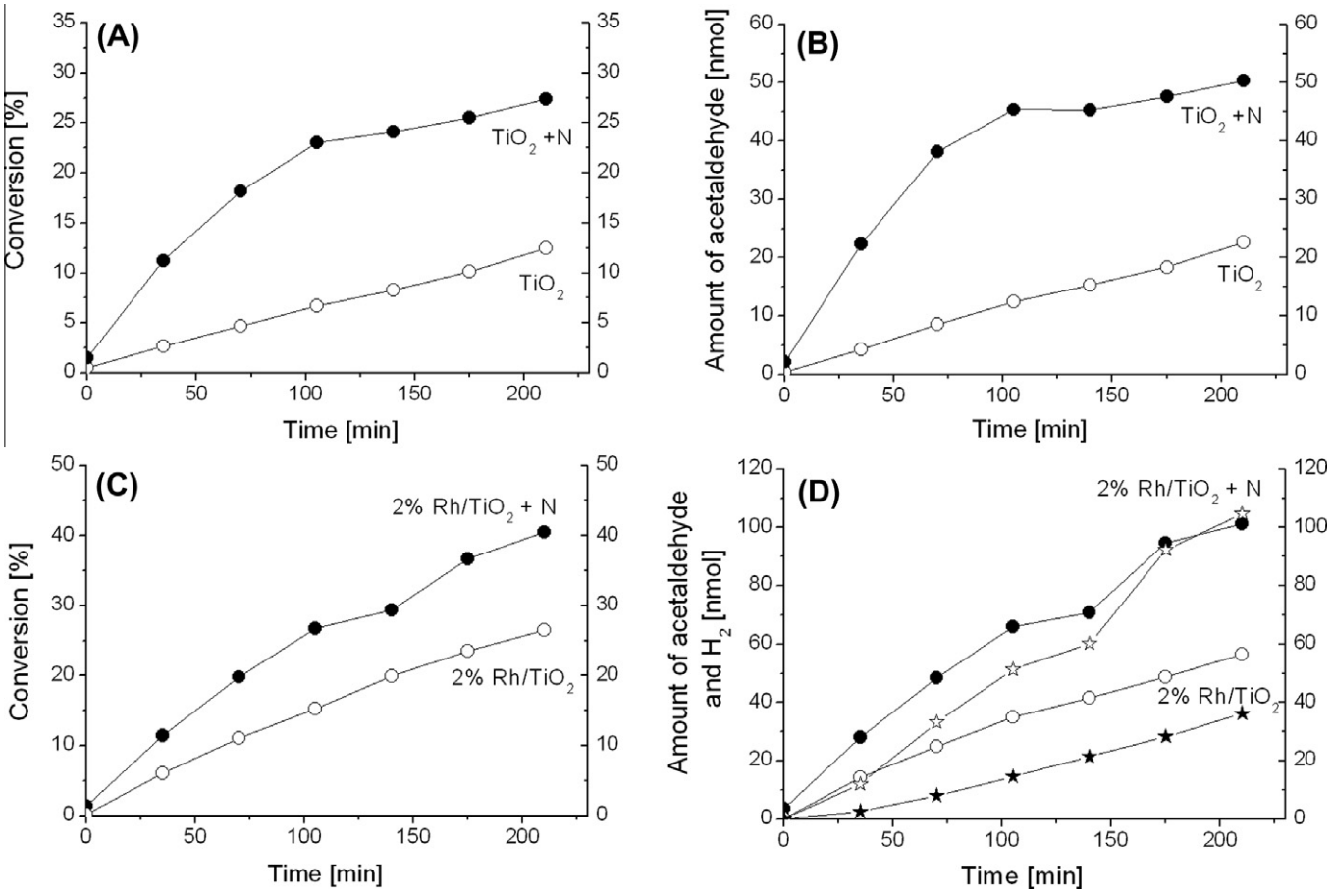

Fig. 6. Effects of N doping of TiO_2 (SX) on the photocatalytic decomposition of ethanol in the visible light on TiO_2 (A and B) and 2% Rh/TiO_2 (SY) (C and D) (★, ☆ H_2; ●, ○ acetaldehyde).

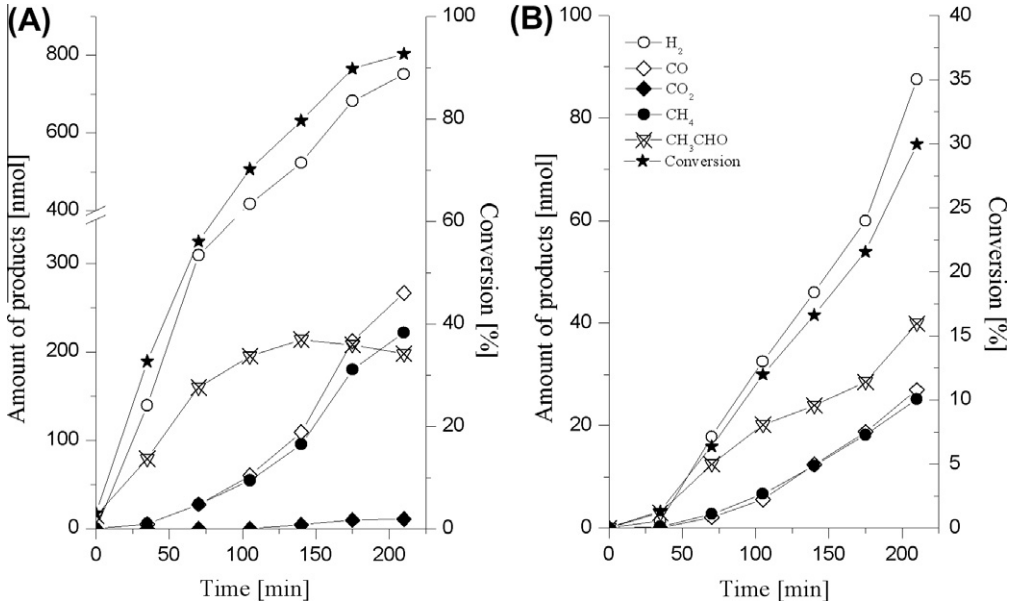

Fig. 7. Conversion and product distribution of the photodecomposition of ethanol on 2% Rh/TiO_2 (A) and 2% Ag/TiO_2 (B).

acid on Ni/TiO_2, when (as far as we are aware) TiO_2 was first used as a support [58,59]. Variation of the electron density or the work function of TiO_2 doping with altervalent cations influenced the activation energy of the decomposition of formic acid. We assume that the illumination enhances the extent of electron transfer from TiO_2 to Rh at the interface of the two solids, leading to increased decomposition. We believe that a similar phenomenon occurs in the case of Ag/TiO_2.

4. Conclusions

(i) On the modification of TiO_2 through incorporation of N species containing carbon, its bandgap is markedly narrowed on elevation of the annealing temperature.
(ii) Doping TiO_2 with N greatly increased its photoactivity in its reaction with ethanol to give acetaldehyde and hydrogen as primary products. The acetaldehyde formed subsequently underwent photolysis to methane and CO.
(iii) The deposition of Rh or Ag on pure or N-doped TiO_2 dramatically enhanced the photodecomposition of ethanol.
(iv) Lowering the bandgap of TiO_2 through N incorporation facilitated the photolysis of ethanol on TiO_2 and Rh/TiO_2 in visible light.

Acknowledgments

This work was supported by the grant OTKA under contract number K 81517. A loan of rhodium chloride from Johnson–Matthey PLC is gratefully acknowledged.

References

[1] G. Sandstede, T.N. Veziroglu, C. Derive, J. Pottier (Eds.), Proceedings of the Ninth World Hydrogen Energy Conference, Paris, France, 1972, p. 1745.
[2] A. Haryanto, S. Fernando, N. Murali, S. Adhikari, Energy Fuels 19 (2005) 2098.
[3] L.F. Brown, Int. J. Hydrogen Energy 26 (2001) 381.
[4] C. Díagne, H. Idriss, A. Kiennemann, Catal. Commun. 3 (2002) 565.
[5] J.P. Breen, R. Burch, H.M. Coleman, Appl. Catal. B Environ. 39 (2002) 65.
[6] D.K. Liguras, D.I. Kondarides, X.E. Verykios, Appl. Catal. B Environ. 43 (2003) 345.
[7] V. Fierro, V. Klouz, O. Akdim, C. Mirodatos, Catal. Today 75 (2002) 141.
[8] V. Klouz, V. Fierro, P. Denton, H. Katz, J.P. Lisse, S. Bouvot-Mauduit, C. Mirodatos, J. Power Sources 105 (2002) 26.
[9] F. Aupretre, C. Descorme, D. Duprez, Catal. Commun. 3 (2002) 263.
[10] F. Marino, G. Baronetti, M. Jobbagy, M. Laborde, Appl. Catal. A Gen. 238 (2002) 41.
[11] J. Llorca, N. Homs, J. Sales, P.R. de la Piscina, J. Catal. 209 (2002) 306.
[12] P.-Y. Sheng, A. Yee, G.A. Bowmaker, H. Idriss, J. Catal. 208 (2002) 393.
[13] A. Erdőhelyi, J. Raskó, T. Kecskés, M. Tóth, M. Dömök, K. Baán, Catal. Today 116 (2006) 367.
[14] M. Dömök, M. Tóth, J. Raskó, A. Erdőhelyi, Appl. Catal. B Environ. 69 (2007) 262.
[15] A.C. Basagiannis, P. Panagiotopoulou, X.E. Verykios, Top. Catal. 51 (2008) 2.
[16] A. Gazsi, P. Tolmacsov, F. Solymosi, Catal. Lett. 130 (2009) 386.
[17] J.R. Salge, G.A. Deluga, L.D. Schmidt, J. Catal. 235 (2005) 69.
[18] R. Barthos, A. Széchenyi, F. Solymosi, Catal. Lett. 120 (2008) 161.
[19] R. Barthos, A. Széchenyi, Á. Koós, F. Solymosi, Appl. Catal. A Gen. 327 (2007) 95.
[20] K. Hauffe, Reaktionen in und an Festen Stiffen, Springer Verlag, Berlin, 1955.
[21] Z.G. Szabó, F. Solymosi, Acta Chim. Hung. 25 (1960) 145.
[22] S. Sato, Chem. Phys. Lett. 123 (1986) 126.
[23] Y. Ukisu, T. Miyadera, A. Abe, K. Yoshida, Catal. Lett. 39 (1996) 265.
[24] R. Asahi, T. Morikawa, T. Ohwaki, K. Aoki, Y. Taga, Science 293 (2001) 269.
[25] J.-H. Xu, W.-L. Dai, J. Li, Y. Cao, H. Li, H. He, K. Fan, Catal. Commun. 9 (2008) 146.
[26] H. Irie, Y. Watanabe, K. Hashimoto, J. Phys. Chem. B 107 (2003) 5483.
[27] O. Diwald, T.L. Thompson, T. Zubkov, Ed.G. Goralski, S.D. Walck, J.T. Yates Jr., J. Phys. Chem. B 108 (2004) 6004.
[28] R. Beranek, H. Kisch, Photochem. Photobiol. Sci. 7 (2008) 40.
[29] P. Romero-Gómez, S. Hamad, J.C. González, A. Barranco, J.P. Espinós, J. Cotrino, A.R. González-Elipe, J. Phys. Chem. C 114 (2010) 22546 (and references therein).
[30] M.R. Hoffmann, S.T. Martin, W. Choi, D.W. Bahnemann, Chem. Rev. 95 (1995) 69.
[31] A. Linsebigler, G. Lu, J.T. Yates Jr., Chem. Rev. 95 (1995) 735.
[32] M. Kitano, M. Matsuoka, M. Ueshima, M. Anpo, Appl. Catal. A Gen. 325 (2007) 1.
[33] G.R. Bamwenda, S. Tsubota, T. Nakamura, M. Haruta, J. Photochem. Photobiol. A: Chem. 89 (1995) 177.
[34] C.-H. Lin, C.-H. Lee, J.-H. Chao, C.-Y. Kuo, Y.-C. Cheng, W.-N. Huang, H.-W. Chang, Y.-M. Huang, M.-K. Shih, Catal. Lett. 98 (2004) 61–66.
[35] N. Strataki, V. Bekiari, D.I. Kondarides, P. Lianos, Appl. Catal. B: Environ. 77 (2007).
[36] Y.Z. Yang, C.-H. Chang, H. Idriss, Appl. Catal. B Environ. 67 (2006) 217.
[37] A. Patsoura, D.I. Kondarides, X.E. Verykios, Appl. Catal. B Environ. 64 (2006) 171.
[38] P.M. Jayaweera, E.L. Quah, H. Idriss, J. Phys. Chem. C 111 (2007) 1764.
[39] Z. Yu, S.S.C. Chuang, J. Catal. 246 (2007) 118 (and references therein).
[40] L. Kőrösi, A. Oszkó, G. Galbács, A. Richardt, V. Zöllmer, I. Dékány, Appl. Catal. B Environ. 77 (2007) 175.
[41] J. Ménesi, L. Kőrösi, É. Bazsó, V. Zöllmer, A. Richardt, I. Dékány, Chemosphere 70 (2008) 538.
[42] L. Kőrösi, S. Papp, J. Ménesi, E. Illés, V. Zöllmer, A. Richardt, I. Dékány, Coll. Surf. A Physicochem. Eng. Aspects 319 (2008) 136.
[43] X. Fu, D.Y.C. Leung, X. Wang, W. Xue, X. Fu, Int. J. Hydrogen Energy 36 (2011) 1524.
[44] D. Meroni, S. Ardizzone, G. Cappelletti, C. Oliva, M. Ceotto, D. Poelman, H. Poelman, Catal. Today 161 (2011) 169.
[45] A. Abe, N. Aoyama, S. Sumiya, N. Kakuta, K. Yoshida, Catal. Lett. 51 (1998) 5.
[46] T. Chadik, S. Kaweoka, Y. Ukisu, T. Miyadera, J. Mol. Catal. A Chem. 136 (1998) 203.
[47] N. Bion, J. Saussey, M. Haneda, M. Daturi, J. Catal. 217 (2003) 47 (and references therein).
[48] Gy. Halasi, A. Kecskeméti, F. Solymosi, Catal. Lett. 135 (2010) 16.
[49] J.I. Pankove, Optical Processes in Semiconductors, Prentience-Hall Inc., New Jersey, 1971.
[50] H. Tang, K. Prasad, R. Sanilines, P.E. Schmid, F. Levy, J. Appl. Phys. 75 (1994) 2042.
[51] F. Solymosi, T. Bánsági, J. Phys. Chem. 83 (1979) 552.
[52] F. Solymosi, M. Pásztor, J. Phys. Chem. 90 (1986) 5312.
[53] S. Sakthivel, M.V. Shankar, M. Palanichamy, B. Arabindoo, D.W. Bahnemann, V. Murugesan, Water Res. 38 (2004) 3001.
[54] M.C. Hidalgo, M. Maicu, J.A. Navío, G. Colón, Appl. Catal. B Environ. 81 (2008) 49.
[55] M.C. Hidalgo, M. Maicu, J.A. Navío, G. Colón, J. Phys. Chem. C 113 (2009) 12840.
[56] F. Solymosi, A. Erdőhelyi, T. Bánsági, J. Catal. 68 (1981) 371.
[57] I. Tombacz, F. Solymosi, Catal. Lett. 27 (1994) 61.
[58] Z.G. Szabó, F. Solymosi, in: Proceedings 2nd International Congress on Catalysis, Technip, Paris, 1961, p. 1627.
[59] F. Solymosi, Catal. Rev. 1 (1967) 233.